Charged Particle Emission during Electron Beam Excitation of Deuterium Subsystem in Pd and Ti- Deuteride Targets

Andrei Lipson[1], Ivan Chernov[2], Alexei Roussetski[3], Yuri Chardantsev[2], Boris Lyakhov[1], Eugeny Saunin[1] and Michael Melich[4]

[1] *A.N. Frumkin Institute of Physical Chemistry and Electrochemistry, Russian Academy of Sciences, 119991 Moscow, Russia*

[2] *Tomsk Polytechnic University, 634050 Tomsk, Russia*

[3] *P. N. Lebedev Physics Insitute, Russian Academy of Sciences, 119991 Moscow, Russia*

[4] *Naval Postgraduate School, Monterey, CA 93943-5000 USA*

Abstract

Energetic charged particle emissions accompanying deuterium desorption from specially prepared Pd/PdO:Dx and TiDx targets in vacuum, stimulated by electron beam (J ~ 0.6 mA/cm2, U = 30 keV) have been studied using a set of CR-39 plastic track detectors covered with various metal foil filters. It was found that the electron bombardment of those targets is caused by statistically significant emissions of DD-reaction product (3 MeV protons), as well as high energy alpha particles (11-20 MeV). At the same time the Pd/PdO:Dx and the TiDx samples show no sign of nuclear emissions during vacuum exposure without e-beam stimulation. Extrapolation of both the DD-reaction cross section and the enhancement factor (consistent with calculated screening potential U_e = 750 eV) to very low deuteron energy allowed us to satisfactorily describe the detected DD-reaction yield in Pd/PdO:D_x target, assuming "hot" deuteron (E_d ~ 3.0 eV) generation under e-beam bombardment. This result strongly supports the theoretical prediction [1,2] with regards to electron excitation of the D- subsystem in Pd- deuterides

1. Introduction

Recent *ab-initio* theoretical studies of hydrogen desorption from metal hydrides/deuterides with a high hydrogen solubility have shown that excitation of the hydrogen subsystem in those deuterides results in plasmon formation leading to electron density oscillations producing a strong electric field (F ~ 10^8 V/cm) within a lattice parameter scale (a ~ 0.3-0.4 nm) [1,2]. As a result, a mean energy of desorbed protons/deuterons (E_d), escaping from the hydride surface would effectively be increased from kT to the several eV values (E_d = F×a ~ 3-4 eV) or two orders of magnitude, effectively producing "hot" deuterons. This deuteron acceleration mechanism, alongside a possible large electron screening in the metal targets with high hydrogen diffusivity [3-5] could potentially strongly enhance the yield of DD-reaction in metal deuterides, even at the extremely low energy of their excitation. In order to verify the hypothesis on the role of excitation of the hydrogen subsystem in metal deuterides to enhance the yield of low energy nuclear reactions (LENR), we have carried out a series of experiments

on charged particle detection with plastic track detectors CR-39, using electron-beam (in vacuum) stimulation of various metal deuterides during spontaneous deuterium desorption (if any) from the deuterated samples.

Here we show that electron beam stimulation of the D-desorption process from specially prepared Pd/PdO:Dx and TiDx targets is caused by statistically significant emissions of DD-reaction product (3 MeV protons), as well as high energy alpha particles. It is important that the same Pd/PdO:Dx and TiDx samples show no sign of nuclear emissions in vacuum without e-beam stimulation. Extrapolation of both DD-reaction cross section and the enhancement factor (consistent with calculated screening potential U_e = 750 eV) to very low deuteron energy (E_d ~ 1.0 eV) allowed to describe satisfactorily the detected DD-reaction yield in Pd/PdO:D_x target under e-beam excitation. This result strongly supports the theoretical prediction [1,2] with regards to electron excitation of the D- subsystem in Pd/PdO deuteride.

2. Experimental

The experiments with e-beam stimulation have been performed in TPU, Tomsk. The samples for the experiments were synthesized in the Frumkin Insitute of RAS. The Pd-based samples were prepared from Nilaco (Japan) Pd foil (99.95% purity) of 50 μm thick with dimensions S = 30 × 10 mm^2. The TiD_x samples were prepared from laboratory grade pure titanium foils of 30 and 300 μm thick. The Pd/PdO heterostructure samples served as cathodes during their electrochemical loading in 0.3 M-LiOD solution in D_2O with a Pt anode. The loading has been carried out at j = 10 mA/cm^2 at ~ 280 K (below room temperature) in a special electrolytic cell with split cathode and anodic spaces. After the loading up to x = D/Pd ~ 0.73 (about 40 min required) the samples were rinsed in pure D_2O and then were put in the Dewar glass to cool them down to T =77 K. Those cooled samples were then rapidly mounted (during 1 min) in sample holder in front of two or three CR-39 detectors covered with various metal foils (filters) and put in a vacuum chamber of SEM using a special handle-manipulator (Fig. 1). In the first series of experiments the e-beam bombarded the sample in one fixed position in the center (the scanning has been carried out within the beam spot). In the second series of experiment, it was possible to move e-beam along the sample surface in three fixed position, producing 15 min irradiation in each position. The mean fraction of the deuterium desorbed from the sample during e-beam irradiation in vacuum has been determined by anodic polarization of the samples after termination of the irradiation. This measurement showed about 10% of residual deuterium remaining in the Pd/PdO:Dx sample after its 50 min of 30 keV e-beam irradiation with current density J= 0.6 μA/cm2. This desorption rate is consistent with a mean D+ desorption current from the Pd/PdODx sample during e-beam action $J_D \sim 3.3 \times 10^{15}$ D/s-cm^2. This number of desorbed deuterons is consistent with the rate of D-desorption in air at ambient conditions (Fig. 1).

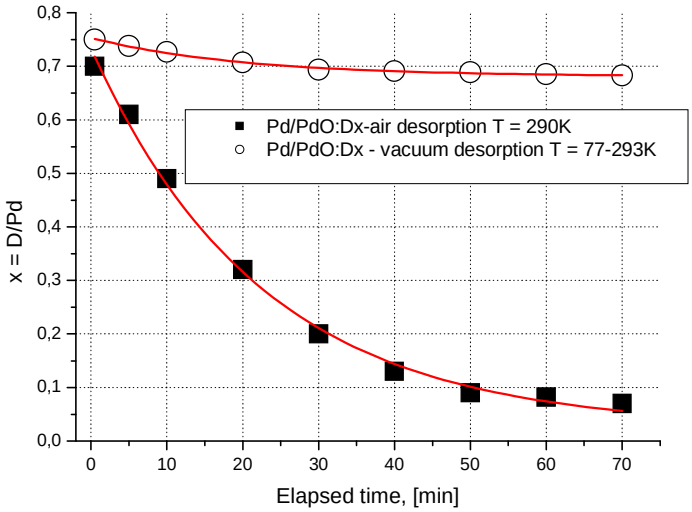

Figure 1. D-desorption rate from the Pd/PdO:Dx samples in vacuum (electrolysis at T=280 K with cooling down to T = 77K after electrolysis termination)) and in air at ambient conditions (electrolysis at T=290K).

In contrast to Pd/PdO samples, the Ti samples have been loaded in a 1 M solution of D_2SO_4 in D_2O during t = 35 hr at J = 30 mA/cm^2, in order to dissolve the TiO_2 oxide layer at the Ti-surface and to provide D-penetration. This technique is able to provide TiD_1 compound formation at the Ti cathode surface layer of several microns thick. The average loading here has been determined by weight balance of the sample before and after e-beam irradiation. It was found that the D-desorption rate in case of TiD irradiation is consistent with the $J_D \sim 1.0 \times 10^{14}$ D/s-cm^2. Important that TiD_1 compound is very stable and does not loose deuterium below t = 400 C. Thus, all desorbed deuterons in TiD has been caused only by e-beam irradiation.

The set of noiseless plastic track detectors has been used to detect charged particles emitted during exposure of deuterated samples under electron excitation. In order to identify type and energy of emitted particles we used simultaneously two or three CR-39 detectors covered with various foils with known stopping ranges (this arrangement can be considered as a simple dE-E detector without a temporal data channel). Similar reference experiments were performed in the Frumkin Institute. These were carried out in vacuum with open and Cu-covered CR-39 detectors, but with no electron beam excitation.

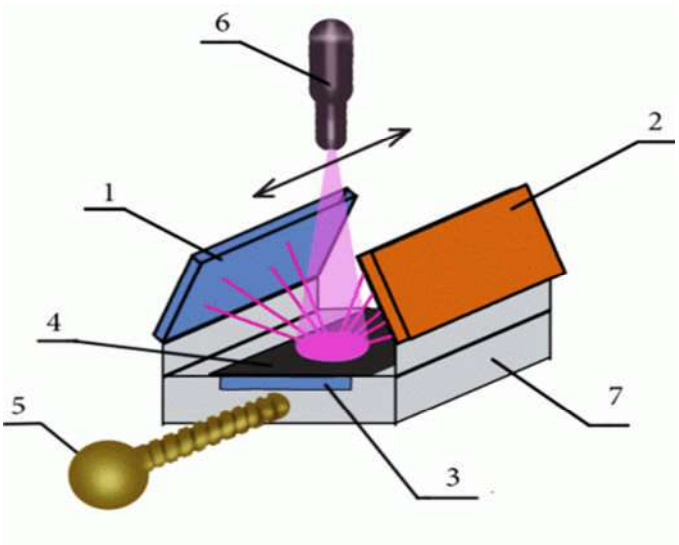

Figure 2. Experimental sample-detector holder mounted in the SEM vacuum chamber ($p = 10^{-6}$ torr) and irradiated by collimated electron beam of EDS electron gun (J = 100-300 nA, E = 30 keV): where 1,2 and 3 – are the CR-39 detectors covered with the 11 μm Al (1), 25 μm Cu (2) and 33 μm Al (3) foil filters, respectively, 4 – is the deuterated sample. 5-manipulator, 6-electron gun, 7- stainless steel support

The desorbed deuterium and generated charged particles reach the detectors from the spot produced by e-beam with dimensions $S = 8 \times 6$ mm^2. The effective distance between the center of the spot and the detectors 1 and 2 is about $<R_{eff}> = 12$ mm. The background counts are always taken from the rear side of CR-39 (opposite to the side directed to the sample's surface). The Foreground counts have been read out from the CR-39 surface of detectors 1, 2 and 3 faced the sample, while the background counts have been taken from the rear sides of these same detectors faced to the vacuum chamber (1, 2) or to the stainless support (3). The resulting counts caused by charged particle emission from the sample, were thus derived by subtracting of the background read out data (rear side) from the foreground (the front side faced to the sample) of the same CR-39 detector. The subtracting of the rear side reading data could provide more precise result in case if CR-39 detectors are irradiated by fast neutrons. Unfortunately, this batch of CR-39 track detectors was irradiated by weak fast neutron flux en route to Moscow from USA, most probably in an airport security facility. As a result, the background level in the track diameter range of interest (4-8 μm) was found to be 4-5 times above the usual 4-8 μm track diameter background, which is normally show $N < 10$ track/cm^2.

Only tracks close to the normal incidence (with respect to the CR-39 surface, such that incidence angle with respect to the perpendicular to the detector's surface would be $\Theta = 0 \pm 10°$). The effective read out area of the CR-39 detector chips with dimensions 2x1 cm^2 was normally of 1 cm^2 (to avoid severely defective edge detector's sites).

In such a condition the effective geometrical efficiency of the detectors 1 and 2 was calculated as following: $\varepsilon_g = 1/4\pi<R_{eff}>^2 S = 2.6 \times 10^{-2}$, where $S = 0.48$ cm^2 is the effective area of the irradiated spot at the surface of the sample, which is taken equal to the area of the e-beam.

Earlier we showed that the efficiency of the detectors that are in tight contact with sample (the #3 detector case) is calculated as $\varepsilon \cong \frac{1}{2}(1-\cos\Theta_c)$, where Θ_c is the critical angle for charged particle of the given type and energy, the $\varepsilon \sim 1/2$ is the numerical coefficient counting for the including into consideration also the "non-circular" tracks, (i.e. the tracks with the small deviations from their circular shape). The detectors were etched in 6 N NaOH at t = 70 C with the rate of ~ 1.3 μ/hr.

The negative results showing absence of the charged particle emissions in the background measurements are shown in Fig. 3.

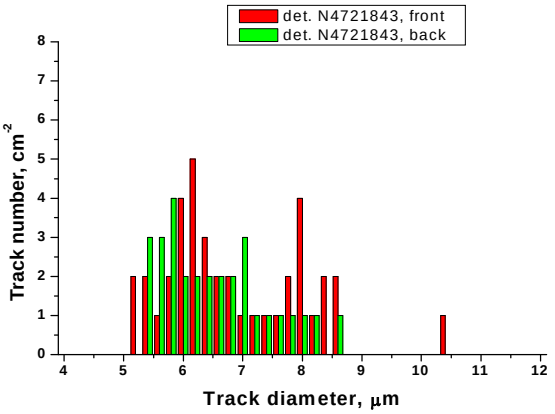

(3a)

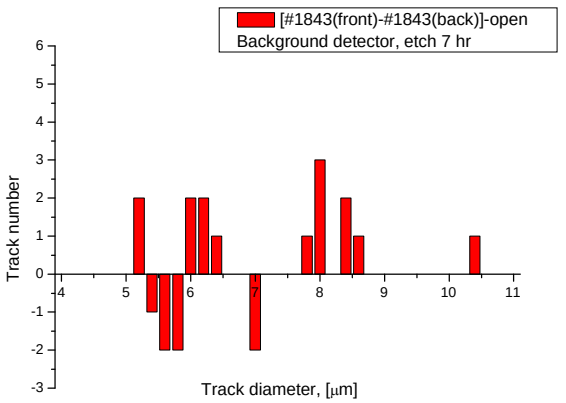

(3b)

Figure 3 a,b background in the vacuum chamber (Tomsk). As seen, in the diameter range of interest (5-8 μm) the deviation of track number difference between the front and the rear side of the detector is about ± 2. The tracks at the detector's surface are due to a weak fast neutron irradiation and radon exposure (see the "maximum" at ∅ = 8 μm).

3.1. Experimental Results: Pd/PdO:D_x

In order to evaluate contribution of the electron beam stimulation it was important to carry out CR-39 measurements in the spontaneous vacuum D-desorption mode at T=290 K (upper curve in Fig. 1). To increase efficiency of measurements the detection here has been performed using two detectors (one open, another filtered with 25 μm thick Cu-foil) attached to the Pd/PdODx samples from their both sides. The results presented in Fig. 5 (a-d) show a null effect.

3.1.1. Pd/PdO:Dx exposure without e-beam stimulation: no proton and alpha effects

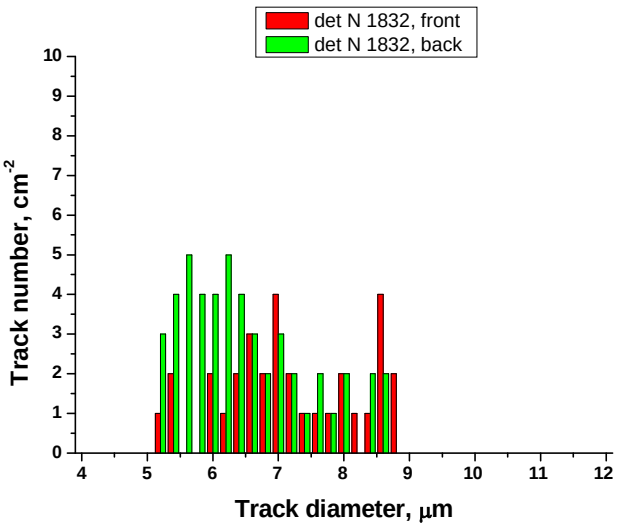

Figure 4a: Open detector results- the front and the back sides counts

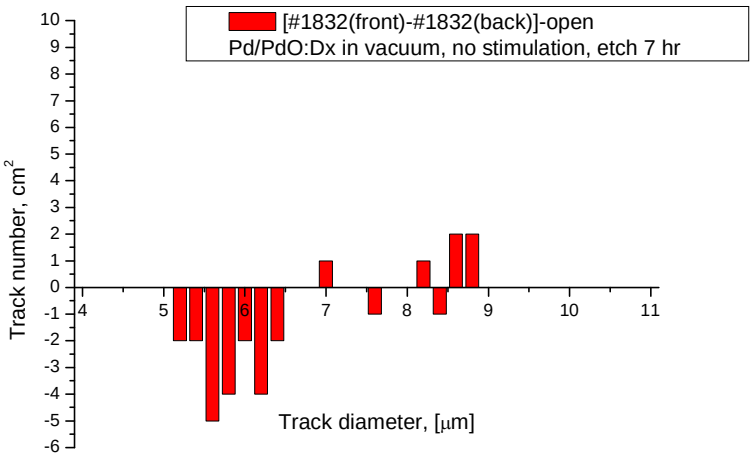

Figure 4b: Open detector- the difference between the front (attached to the sample) and back (i.e. opposite to the front one) sides of the CR-39 detector.

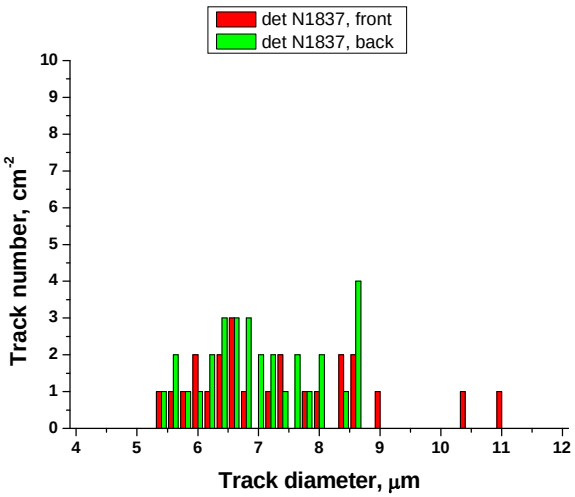

Figure 4c. 25 μm Cu covered CR-39 detector results: - the front and the back sides counts

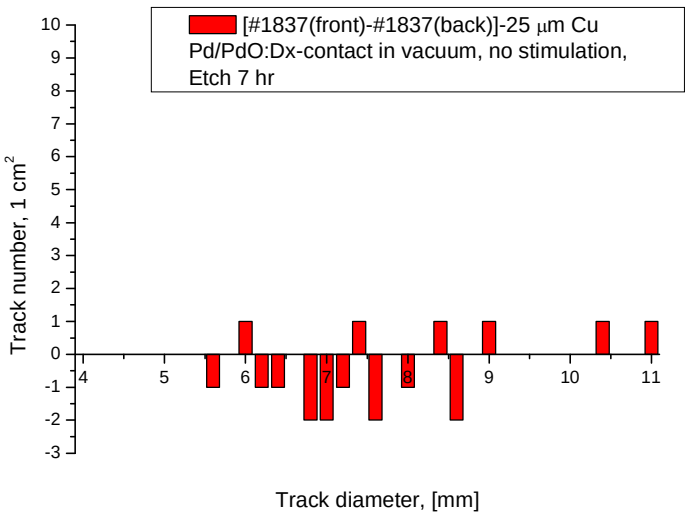

Figure 4d. 25 μm Cu covered CR-39 detector; the difference between the front (attached to the sample) and back (no contact with the sample, i,e, opposite to the front side) sides of the CR-39 detector

3.1.2. Electron beam irradiation of the Pd/PdO/Pd:D_x

The statistically provided results have been obtained in two separate series of experiments with Pd/PdO/Pd:D_x samples consisting of 16 and 20 runs, respectively exposed in vacuum under electron beam stimulation. In these experiments we used 3 CR-39 detectors in each series (as shown in Fig. 2). Two of them (covered with 11 μm Al and 25 μm Cu foils) have been placed under the free face of the sample irradiated by e-beam; the third detector (covered with

33 μm Al) has been placed at the rear side of the sample that has nor been irradiated by electrons.

The results of the first (16 runs) series containing 16 consecutive runs (the run duration is τ = 50 min) with 4 Pd/PdO:Dx samples irradiated by 30 keV electron beam (J = 0.3 μA/cm2) are shown in Figs. 5-7.

In contrast to the experiments without stimulation carried out with the Pd/PdO:Dx samples, the data obtained in Tomsk using 3 independent CR-39 detectors (the diagram is shown in Fig. 2) showed statistically significant counts of 3 MeV protons from DD-reaction as well as the energetic alphas.

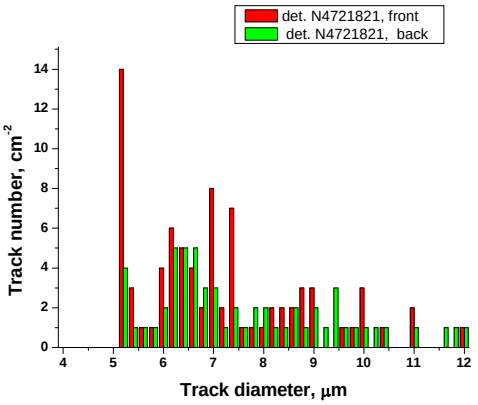

(5a)

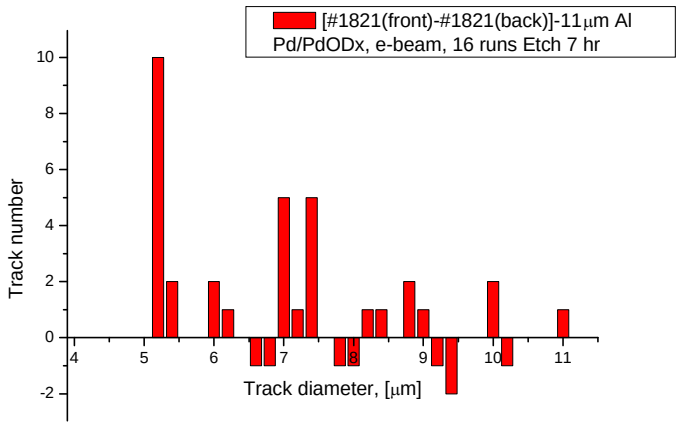

(5b)

Figure 5. a, b. Foreground and background (a) and differential (b) spectra of 11 μm Al covered CR-39 detector (position 1 in Figure 1). Total time of 16 runs with the 4 Pd/PdO:Dx samples is 16 hr. The intensity of 3MeV proton counts (d ~ 5.2 μm), taking into account the detector efficiency is <Np> = (8.0±3) × 10^{-3} p/s-cm^2, The high energy alpha (10<E<16 MeV, d ~ 7-7.4 μm) intensity would be <Nα> = (1.0 ±0.4) × 10^{-2} p/s-cm^2.

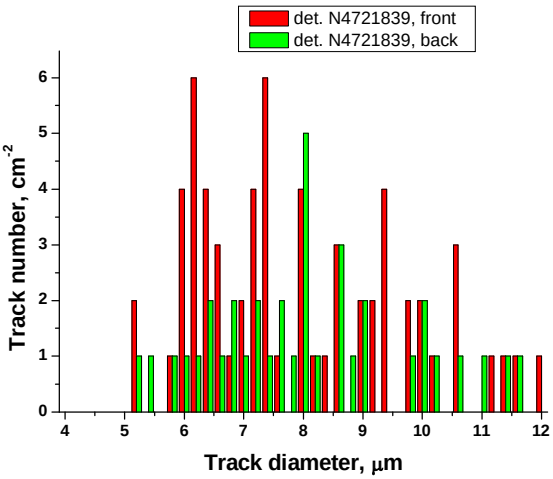

(6a)

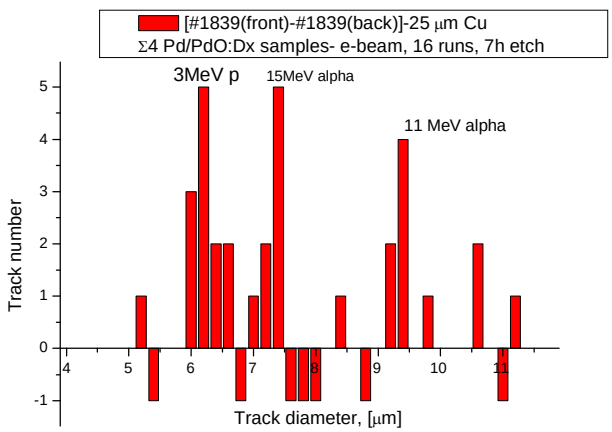

(6b)

Figure 6, a,b. Foreground and background (a) and differential (b) spectra of the 25 μm Cu covered CR-39 detector (position 2 in Figure 1). The intensity of the incident 2.5-3MeV proton counts (d ~ 6.0-6.6 μm), taking into account the detector efficiency is $\langle N_p \rangle = (8.0 \pm 2.6) \times 10^{-3}$ p/s-cm^2; The high energy alpha (incident energies are split in two bands of 12<E<20 MeV, d ~ 7-7.4 μm and 10 < E < 12 MeV d = 9-11 μm) intensity would be $\langle N_\alpha \rangle = (1.0 \pm 0.3) \times 10^{-2}$ α/s-cm^2.

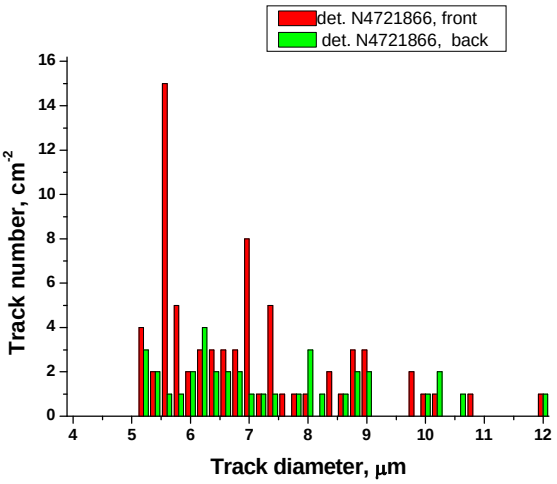

(7a)

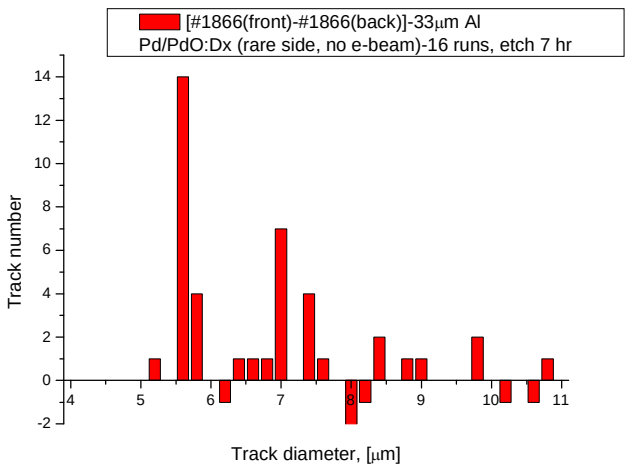

(7b)

Figure 7 a, b. Foreground and background (a) and differential (b) spectra of the 33 μm Al covered CR-39 detector attached to the Pd/PdO:Dx sample from its rear side (position 3 in Figure 1). The intensity of the incident 2.5-3MeV proton counts (d ~ 5.6-5.8 μm), taking into account the detector efficiency (with the critical angle of ~ 35° for 2.1 MeV protons taking into account of 0.9 MeV energy losses of 3.0 MeV protons in 33 μm Al foil) is $<N_p> = (3.5\pm0.9)x\ 10^{-3}$ p/s-cm^2; The high energy alpha (incident energies are split into 12<E<16 MeV, d ~ 7-7.6 μm and 10 < E < 11 MeV d ~10 μm) intensity would be $<N_\alpha> = (1.6 \pm0.6) \times 10^{-3}$ α/s-cm^2.

Even more statistically significant results have been obtained in the second series (20 runs with duration 50 min each) of experiments with 6 freshly prepared Pd/PdO:Dx samples using twice as higher e-beam current (J = 0.6 μA/cm2) as it was in the first series and also producing a scanning of the e-beam along the sample. The results for three detectors (1,2,3 - Fig. 2) and the total sum of the first (16 runs) and second (20 runs) series results are shown below.

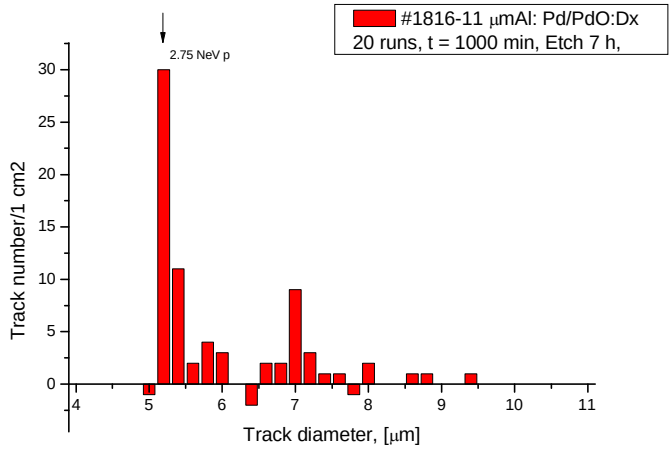

(8a)

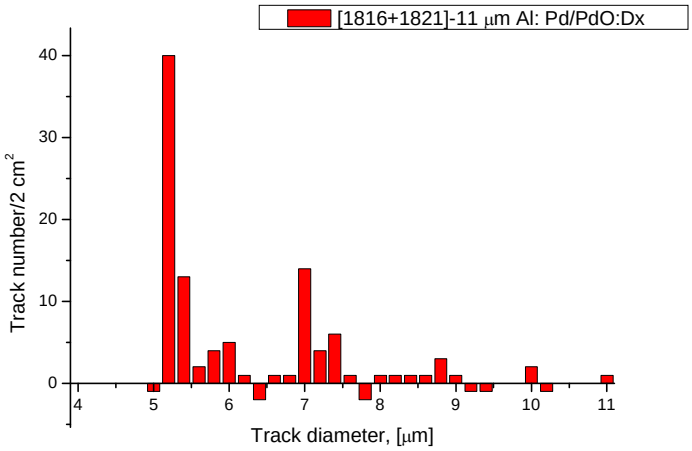

(8b)

Figure 8. a. Differential spectra of the 11 μm Al covered CR-39 detector (position 1 in Figure 2) obtained in the second series (20 runs) of experiments with the 6 Pd/PdODx samples b. The sum obtained in both first (16 runs, Fig. 5b) and second (20 runs) series of experiments. Total time of 1+2 series is τ = 1800 min, using 10 similar Pd/PdO:Dx. As seen both highly statistically significant 2.75 MeV proton (5.2-5.4 μm track diameter) and 11-20 MeV alphas (7.0-7.6 μm track diameter) bands are appeared in the second series of experiments

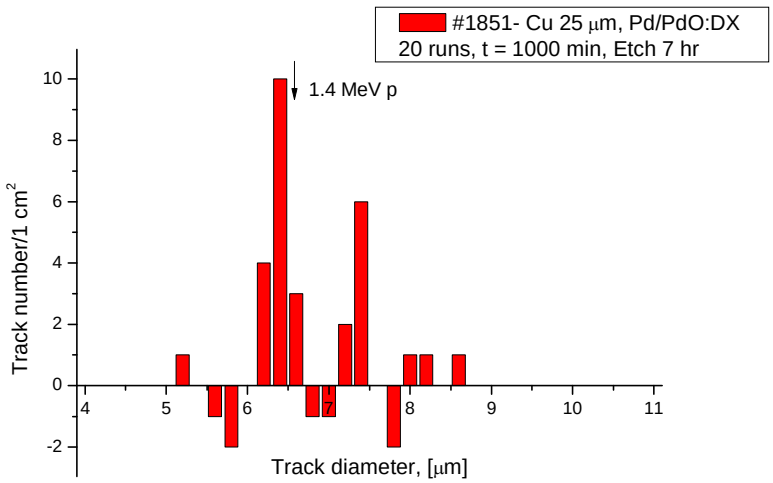

(9a)

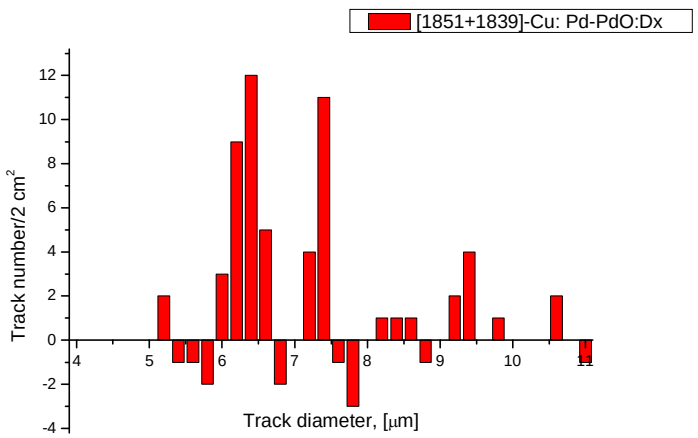

(9b)

Figure 9. a. Differential spectra of the 25 μm Cu covered CR-39 detector (position 2 in Figure 2) obtained in the second series (20 runs) of experiments with the 6 Pd/PdODx samples. b. The sum obtained in both first (16 runs, Fig. 6b) and second (20 runs) series of experiments. Total time of 1+2 series is τ = 1800 min, using 10 similar Pd/PdO:Dx. The statistically significant bands of 1.4 MeV protons (track diameter in the range of 6.0-6.6 μm, consistent with the 3 MeV proton losses in 25 μm Cu foil) and 15 MeV alphas (track diameter near 7.4 μm, consistent with ~ 19 MeV alpha losses in 25 μm Cu foil) are appeared in the sum spectra (b).

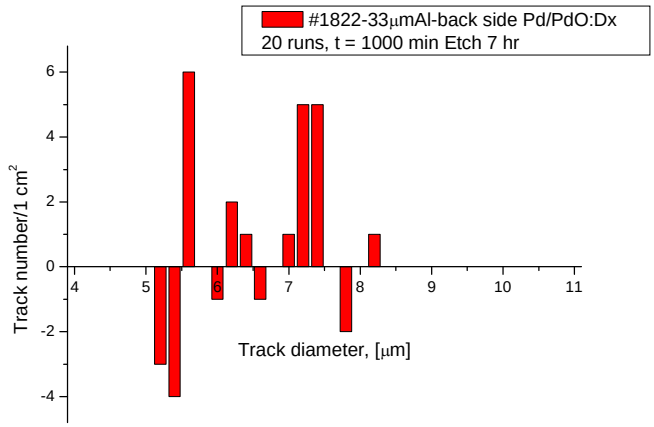

(10a)

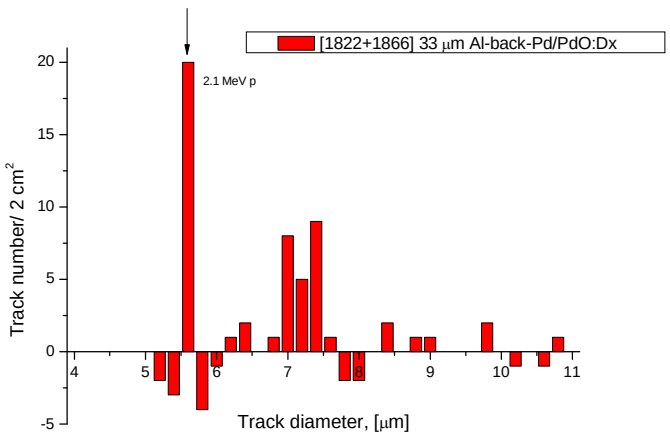

(10b)

Figure 10. a,b Differential spectra of the 33 μm Al covered CR-39 detector placed below the rear (non-irradiated by e-beam) side of the Pd/PdO:Dx sample (the position #3 in Figure 2) obtained in the second series (20 runs) of experiments with the 6 Pd/PdODx samples (a) and the sum obtained in both first (16 runs, Fig. 10 b) and second (20 runs) series of experiments (b). Total time of 1+2 series is τ = 1800 min, using 10 similar Pd/PdO:Dx. The statistically significant bands of 2.1 MeV protons (track diameter near 5.6 μm, consistent with 3 MeV proton losses in 33 μm Al foil) and 14 MeV alphas (track diameter 7-7,4 μm, consistent with ~ 14-19 MeV alpha losses in 33 μm Al foil) are appeared in the sum spectra (b).

3.1.3. Sequential Etching of the Detectors #1 and #2

In order to get additional unambiguous proof that emissions of DD-reaction product (3 MeV protons) and energetic alphas are really observed in our experiments, a sequential etching of the detectors 1 (11 μm Al foil covered, # 1816) and 2 (25 μm Cu foil covered, # 1851) faced to the open surface of the sample (Fig. 2) in the second series of experiment has been performed. This procedure included 14, 21 and 28 hr etching and analysis in addition to the analysis of the same detectors shown in section 3.1.2 for the 7 hr etched detectors. The diameters of tracks obtained

during sequential etching in main peaks (of lower d~ 5.2 μm and higher d ~ 7.0 μm diameter at etch time t=7 hr) have been compared with that of proton and alpha tracks extracted from similarly etched calibration detectors. The sequential etching data for p and α accelerator bombardment are presented in Ref. [6].

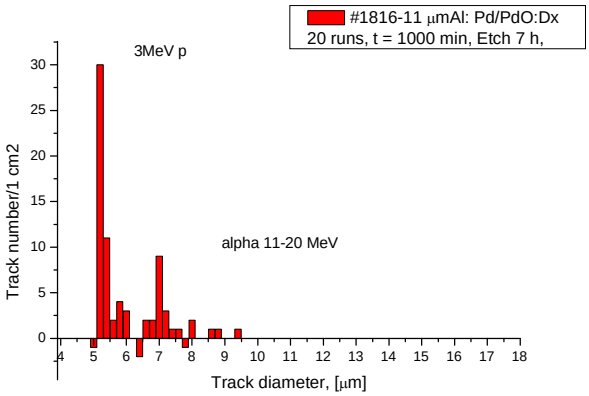

(11a)

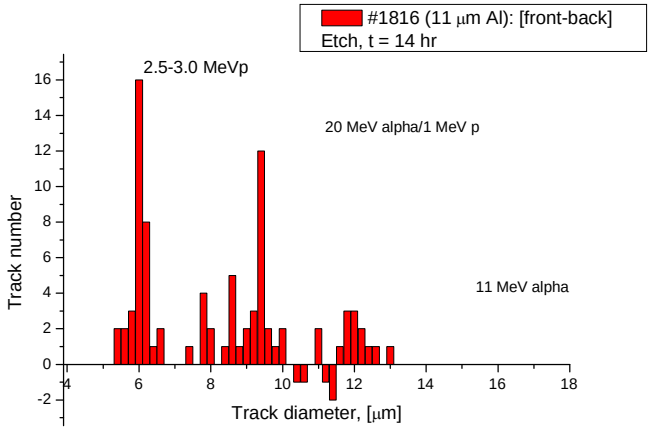

(11b)

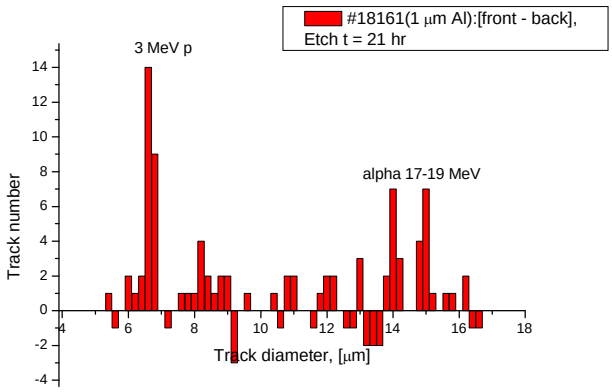

(11c)

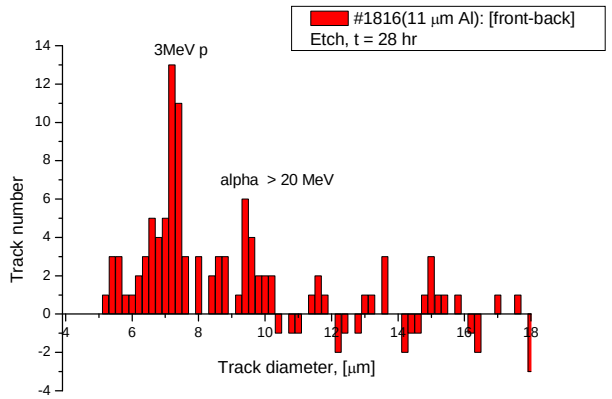

(11d)

Figure 11 (a-d). Differential spectra (with subtracting of the background (the rear detector's face tracks) of #1816 CR-39 detector (exposed during e-beam irradiation of 6 Pd/PdO:Dx samples during 1000 min) after its etching during 7 (a), 14(b), 21(c) and 28(d) hours. The shift of the "peaks" in a larger track diameter side with increase in etching time is well seen.

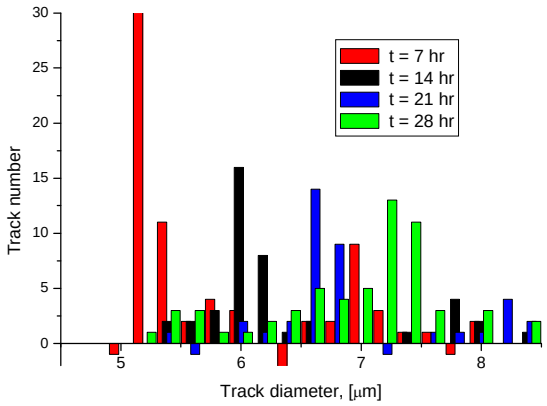

Figure 12. Shift in track diameter for the a main peak (3 MeV protons) obtained during sequential etching of #1816 detector covered with 11 μm thick Al foil

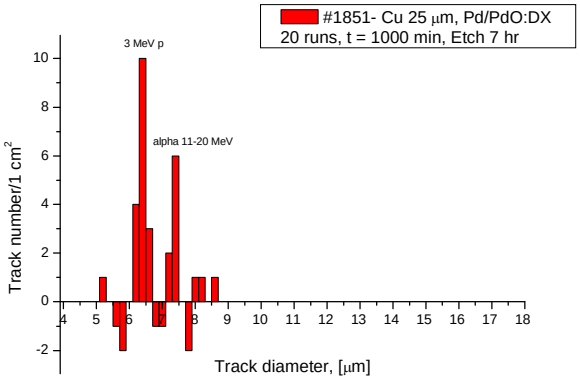

(13a)

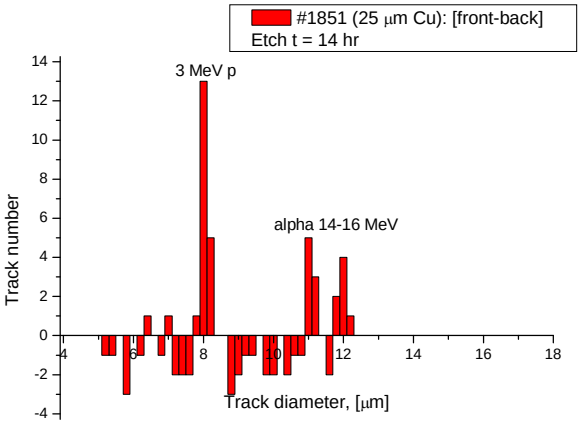

(13b)

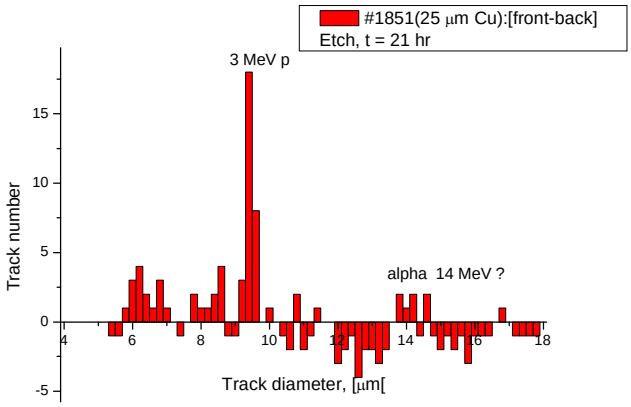

(13c)

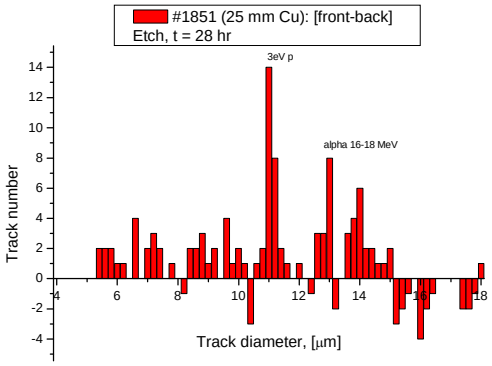

(13d)

Figure 13. Differential spectra (with subtracting of the background rear face results) of #1851 CR-39 detector (exposed in front of the free surface of the 6 Pd/PdO:Dx samples during their e-beam irradiation during 1000 min) after its etching during 7 (a), 14(b), 21(c) and 28(d) hours. The shift of the "peaks" in a larger track diameter side with increase in etching time is well seen.

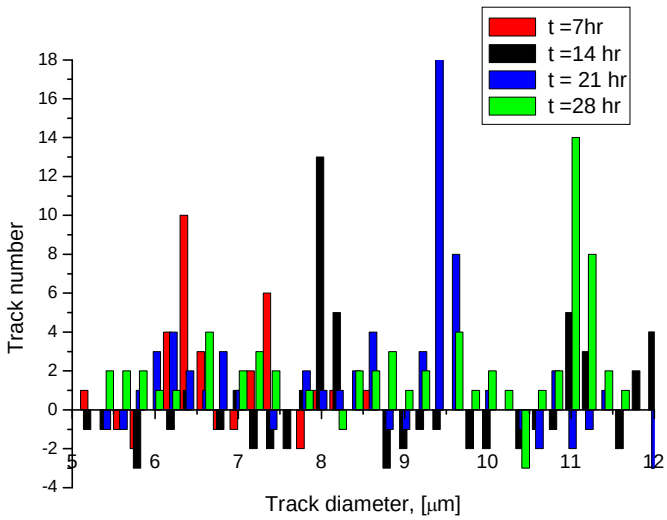

Figure 14. Shift in a main peak track diameter (1.4 MeV protons) following by sequential etching of #1816 detector covered with 25 μm thick Cu foil

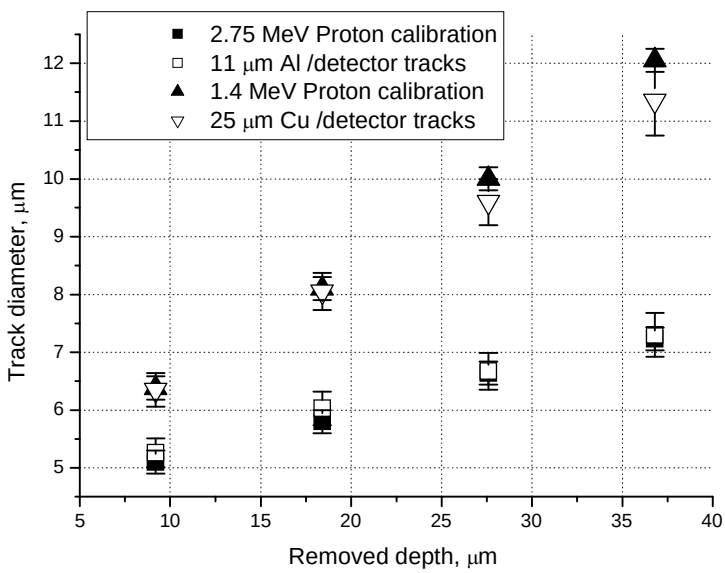

Figure 15. Track diameter vs. removed depth (d(h)) dependences for "proton" tracks detected during sequential etching of the detectors 1 and 2, respectively. The black squares and triangles represent fit of experimental tracks from detectors 1 and 2 (empty squares and triangles, respectively) with d(h) functions obtained using normal incidence accelerator CR-39 bombardment at proton energies 2.75 (consistent with 3 MeV proton after its passage through 11 μm thick Al foil) and 1.4 (consistent with to 3 MeV proton after its passage through the 25 μm thick Cu foil) MeV , respectively.

The sequential etching data (Fig.11-14), including track diameter fit shown in Fig.15 represents an additional unambiguous evidence for 3 MeV proton emission during vacuum electron beam bombardment of the Pd/PdO:Dx heterostructure. Indeed, the shift of tracks in a main (lower diameter track) peak to the larger diameter for both #1 and #2 detectors (Figs. 12 and 14) is consistent (within the standard deviation) with those shifts obtained for 2.75 and 1.4 MeV normal incidence proton tracks, respectively (Fig. 15). Notice that these chosen proton energies of 2.75 and 1. 4 MeV are associated with the 3.0 MeV protons from DD-reaction, passed through the 11 μm thick Al and 25 μm thick Cu foils, respectively. Exactly these foils were used as filters in detector #1 and #2, respectively.

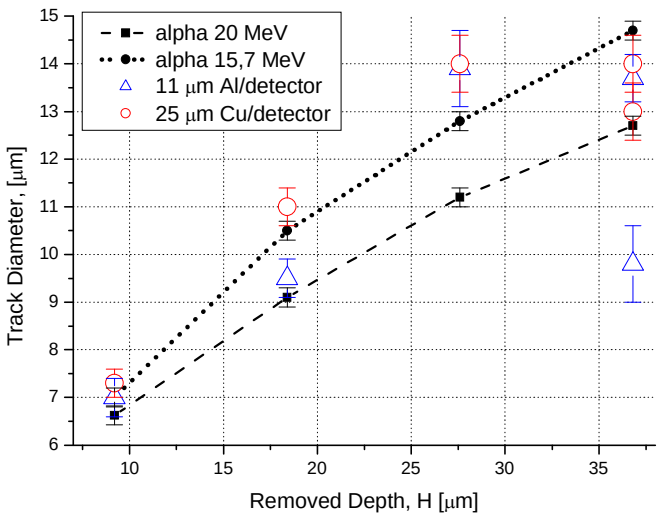

Figure 16. Track diameter vs. removed depth (d(h)) dependences for alpha tracks detected during sequential etching of the detectors 1 and 2, respectively. The dashed and dotted lines represent fits of experimental tracks from detectors 1 and 2 with d(h) functions obtained using normal incidence accelerator CR-39 bombardment at alpha energies 20 and 15.7 (corresponding to 20 MeV alpha after its passage through 25 μm thick Cu foil) MeV, respectively.

Due to lower statistics, the sequential etching data (shown in Figs. 11 and 13) obtained for the second main peak (located at d ~ 7.0-7.6 μm track diameter at etch time t = 7 hr) and their fit with normal incidence accelerator alpha beams of 20 and 15.7 MeV energies (Fig.16) are less impressive than those shown in Fig. 15 for 3.0 MeV protons. The lower statistics of energetic alphas is defined by strong track spread at their larger diameter during CR-39 etching in depth leading to the spread of the second peak. The last circumstance is mainly due to the fact that the emitted alphas do not produce monoenergetic beam, in contrast to DD- protons. The spread is larger at larger track diameter, making it not possible to identify alphas with energy located near 11 MeV.

Despite larger statistical errors (especially with regards to detector 1 covered with 11 μm thick Al foil) in Fig. 16, this data eventually confirm the emission of high energy alphas. Indeed, the track diameter vs. removed depth function d(h) for the detector 2 is satisfactorily

fitted with the d(h) function of 15.7 MeV alphas (Fig. 16 dashed line) At the same time, expecting that alpha particles with mean incident energy of ~ 20 MeV will pass then through the 25 μm thick Cu foil, the energy losses in this foil would be of 4.3 MeV, such that the energy of the alpha-particle decreases to 15.7 MeV. Note that the detector 1 data presented in Fig. 16 could be also fitted with 1.2 MeV proton curve. However in this case one have to expect that Pd/PdO:Dx sample would emit 1.6 MeV protons that are detected by the CR-39 alongside with 3.0 MeV particles. This, however, cannot be occurred because the 25 μm thick Cu foil covering the detector 2 will stop all protons with the energies E < 2.4 MeV. This is why the tracks obtained in the second main peak should only be considered as high energy alpha particles in the range of 11-20 MeV, and cannot be ascribed to 1-2 MeV protons.

Thus, the sequential etching data shows that during e-beam irradiation of the Pd/PdO:D_x heterostructure the 3 MeV protons and high energy alphas (in the range, roughly of 11-20 MeV) really have been emitted.

3.1.4. Charged particle emission rate in the Pd/PdO:D_x

The results for e-beam irradiated face of the Pd/PdO:Dx heterostructure sample, obtained by averaging of 11 μm Al and 25 μm Cu data, taken for detectors 1 and 2 respectively in total 36 runs (t = 1800 min) are following:

- **a.** For 3 MeV protons $\langle \Delta N_p \rangle = (3.71 \pm 0.48) \times 10^{-4}$ cps/cm^2 of CR-39, or taking into account total efficiency of the detection ($\varepsilon = 0.026$) $N_p = (1.39 \pm 0.18) \times 10^{-2}$ p/s-cm^2 of Pd/PdO:Dx sample. (the significance level above the background is L = 7.7 σ)
- **b.** For alpha particles with the energy in the range of 11-20 MeV. $\langle \Delta N_\alpha \rangle = (1.87 \pm 0.32) \times 10^{-4}$ cps/cm^2 of CR-39 or taking into account total efficiency of the detection ($\varepsilon = 0.026$), $N_\alpha = (0.71 \pm 0.12) \times 10^{-2}$ α/s-cm^2 of Pd/PdO:Dx sample. (the significance level is L = 6.0 σ)

The yield of DD-reaction in the Pd/PdO:Dx target under e-beam bombardment, taken only for movable deuterons (the desorbed flux $J_d = 3x10^{15}$ D/s-cm2) is found to be $\lambda_{DD} \sim 3.3x10^{-18}$ p/D.

For the detector in position #3 (Fig 2) placed under the rear (non-irradiated by e-beam) side of the Pd/PdO:Dx sample the average result in total 36 runs (t = 1800 min) during e-beam irradiation of the front side of the Pd/PdO:Dx:

- **a.** For 3 MeV protons $\langle \Delta N_p \rangle = (1.81 \pm 0.40)x\ 10^{-4}$ cps/cm^2 of CR-39, or taking into account total efficiency of the track detection for 1.9 MeV protons after permeation of 3 MeV p through 33 μm Al ($\varepsilon = 0.11$), $N_p = (1.68 \pm 0{,}37) \times 10^{-3}$ p/s-cm^2 of the Pd/PdO:Dx sample. (significance L = 4.5 σ)
- **b.** For alpha particles with the energy in the range of 11-19 MeV $\langle \Delta N_\alpha \rangle = (2{,}49 \pm 0.45) \times 10^{-4}$ cps/cm^2 of CR-39 or taking into account total efficiency of the track detection for high energy (> 11 MeV) alphas ($\varepsilon = 0.17$) $N_\alpha = (1.46 \pm 0.27) \times 10^{-3}$ α/s-cm^2 of the Pd/PdO:Dx sample. (significance L = 5.5 σ).

The count rate calculation results show that the front side of the sample irradiated by electron beam provides an excess (5-8 times) in the absolute intensity of the proton and alpha emissions compared to that detected at the rear side of the sample, which has not been irradiated directly. At the same time both the front and the rear side of the Pd/PdO:Dx sample under e-beam stimulation show a large excess in the proton and alpha emission bands, compared to the same Pd/PdO:Dx target that have been run in vacuum without excitation of their D-subsystem (i.e. in the spontaneous D-desorption mode). Observation of nuclear emissions from the rear side of the target, under e-beam irradiation of its front side, indicates some D-desorption enhancement in vacuum also at the rear side of the e-irradiated Pd/PdO:Dx sample

3.2. Experimental Results: TiD_x

Experiments with the **TiD_x** samples have been carried out similarly to that performed with Pd/PdO:Dx. In contrast to Pd/PdO heterostructure, ready-to- use Ti deuteride samples were put in vacuum chamber. The one surface of the samples have been scanned by electron beam (J = 0.6 μA/cm2). Then in other run the sample has been turned around and the other surface of the TiDx was scanned too. In total there were carried out 26 runs with duration of 50 min each. (total Foreground time is 1300 min, including 300 min (6 runs) in first series and 1000 min (20 runs) in a second series). Three CR-39 detectors (with 11 and 33 μm Al filters and with 26 μm Cu filter), accordingly to diagram depicted in Fig. 2 were used in each series of experiments with the TiDx.

The results on nuclear particle detection for CR-39 covered with Al and Cu filters are shown below.

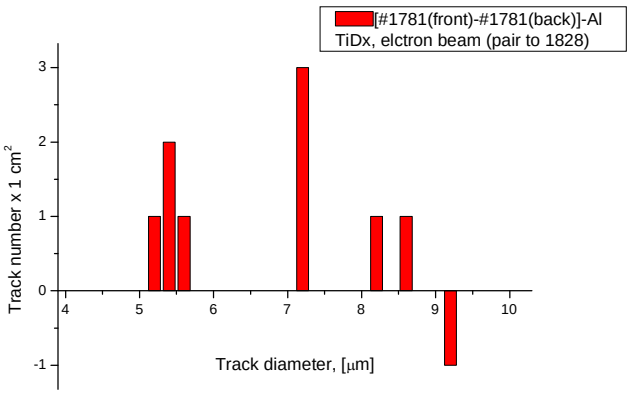

(17a)

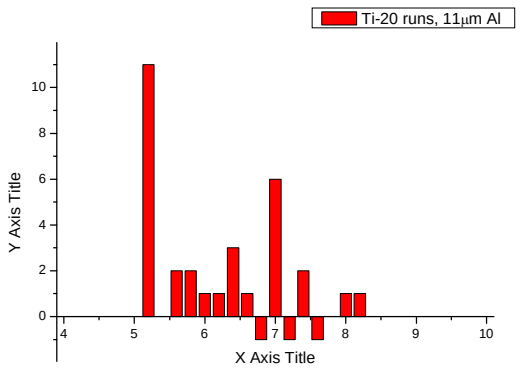

(17b)

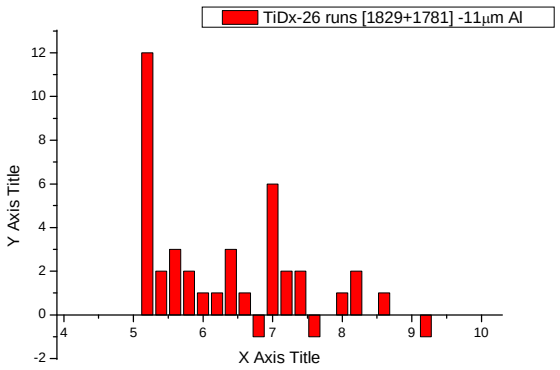

(17c)

Figure 17. a-c Differential spectra of the 11 μm Al covered CR-39 detector (position 1 in Figure 2) obtained in the first series (6 runs) of experiments with the 5 TiDx samples (a), the similar data obtained in the second series (20 runs) of experiment with the TiDx results (b) and the sum obtained in both first (6 runs) and second (20 runs) series of experiments (c). Total time of 1+2 series is τ = 1300 min, using 10 similar TiDx samples. As seen from the data (c), both statistically significant 3 MeV proton (5.2-5.4 μm track diameter) and 11-19 MeV alphas (7.0-7.6 μm track diameter) bands are appeared in the TiDx-electron beam excitation experiments.

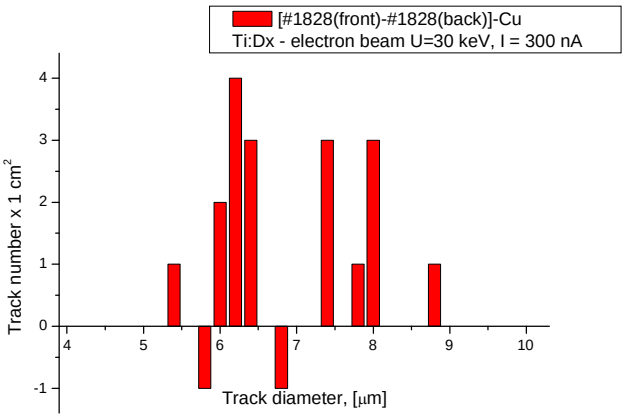
[#1828(front)-#1828(back)]-Cu
Ti:Dx - electron beam U=30 keV, I = 300 nA
Track number x 1 cm^{-2}
Track diameter, [μm]

(18a)

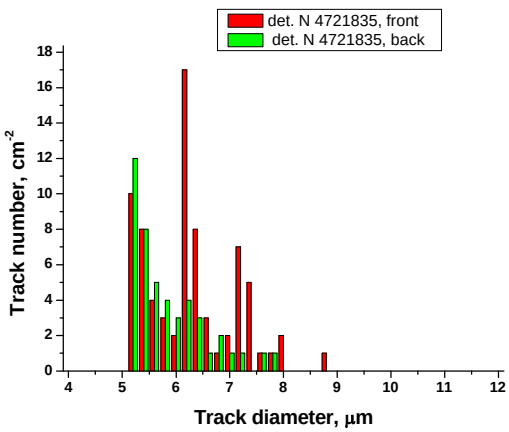
det. N 4721835, front
det. N 4721835, back
Track number, cm^{-2}
Track diameter, μm

(18b)

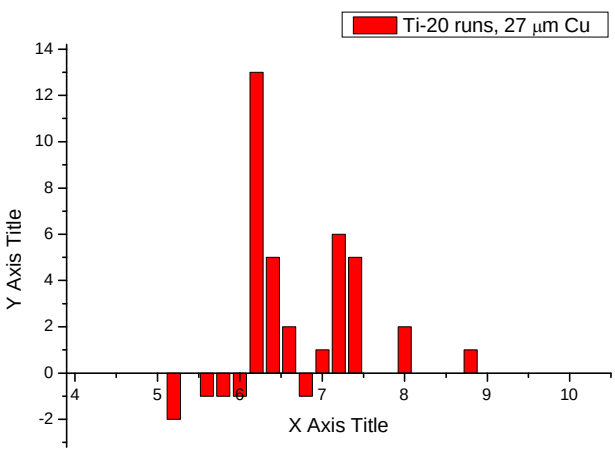
Ti-20 runs, 27 μm Cu
Y Axis Title
X Axis Title

(18c)

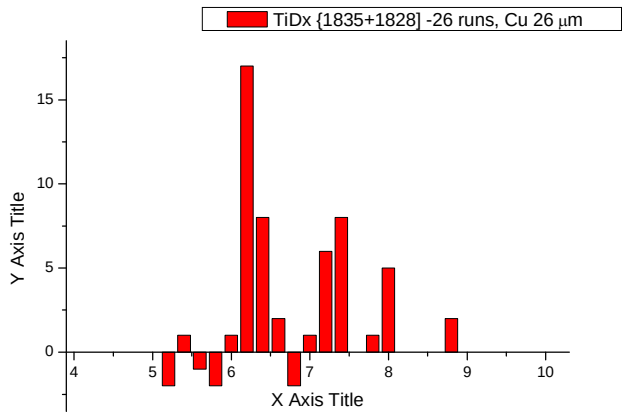

(18d)

Figure 18(a-d) The spectra of the 25 μm Cu covered CR-39 detector (position 2 in Figure 2) obtained in the first series (6 runs) of experiments with the 5 TiDx samples (a); Foreground and background (b) and differential (c) spectra obtained in the second series (20 runs) experiments ; the summary spectrum for total 26 runs obtained by summarizing the spectrum (a) and the spectrum (c). The statistically significant bands of 1.5 MeV protons (track diameter in the range of 6.0-6.6 μm, consistent with the 3 MeV proton losses in 26 μm Cu foil) and 14 MeV alphas (track diameter near 7.4 μm, consistent with ~ 17 MeV alpha losses in 25 μm Cu foil) are appeared in the sum spectra (b).

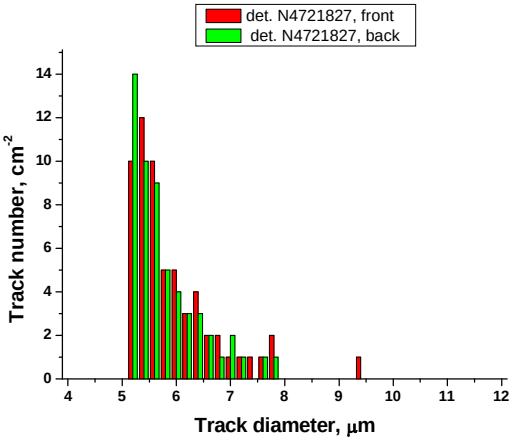

(19a)

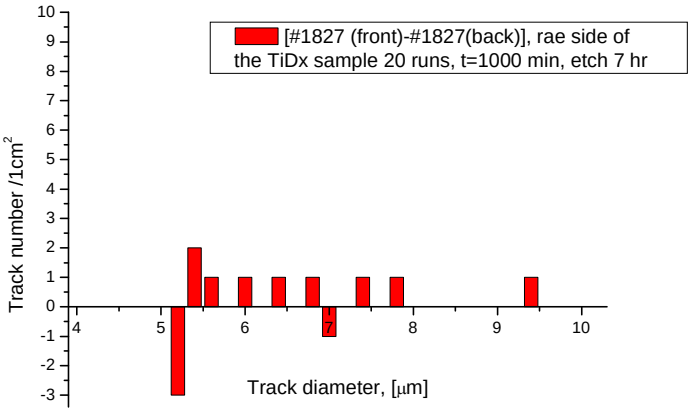

(19b)

Figure 19. a,b The Foreground and the background spectra (a) and the differential spectrum (b) of the 33 μm Al covered CR-39 detector placed below the rear (non-irradiated by e-beam) side of the TiDx sample (the detector with the position #3 in Figure 2) obtained in the second series (20 runs) of experiments with the 5 TiDx samples. No statistically significant results have been found over all differential spectrum (b) of the rear side of the TiDx sample.

The results for e-beam irradiated face of the TiDx sample, obtained by averaging of 11 μm Al and 25 μm Cu data, taken for detectors 1 and 2 respectively in total 26 runs (t = 1300 min) are following:

- **a.** For 3 MeV protons $<\Delta N_p>$ = (2.87 ± 0.61) × 10^{-4} cps/cm^2 of CR-39, or taking into account total efficiency of the detection (ε = 0.026) N_p = (1.10 ± 0.23) × 10^{-2} p/s-cm^2 of TiDx sample. (the significance level of the result above the background is L = 4.74 σ)
- **b.** For alpha particles with the energy in the range of 11-19 MeV $<\Delta N_\alpha>$ = (1.60 ± 0.38) × 10^{-4} cps/cm^2 of CR-39 or taking into account total efficiency of the detection (ε = 0.026), N_α = (0.61 ± 0.15) × 10^{-2} α/s-cm^2 of the TiDx sample (the significance level is L = 4.3 σ).

The non-irradiated by e-beam face of the TiDx sample show no signatures of nuclear emission.

The yield of DD-reaction in the TiDx target under e-beam bombardment, taken only for movable deuterons (the desorbed flux J_d = 10^{14} D/s-cm^2) is found to be λ_{DD} ~ 1.1x10^{-16} p/D.

Thus, the e-beam excitation of the TiDx samples results in initiation of DD-reaction (producing 3 MeV protons) as well as high energy alpha particles. The intensity of the nuclear emissions is quite comparable to that of the Pd/PdO:Dx samples, but provide lower statistical significance. In contrast to Pd/PdO:Dx system the TiDx samples show no emissions from the face opposite to the e-beam irradiated side. This only proofs that no nuclear emissions occur without D-desorption from the rear face of the TiDx samples, while the Pd/PdO:Dx

heterostructure provides weak spontaneous D-desorption from its rear side. Such a desorption could be partially stimulated by e-beam interaction with the front (irradiated) face of the Pd/PdO:Dx sample.

4. Discussion

Thus, we have shown experimentally that charged particle emission in Pd/PdO:Dx abd TiDx in vacuum can be stimulated by relatively weak (J< 1 μA/cm2, E=30 keV) electron beam. We found that e-beam excitation of D-subsytem in those deuterides with a high affinity to hydrogen is resulted in origination of DD-reaction (3 MeV proton emission) as well as energetic alpha particles with energies in the range of 11-19 MeV. The yield of DD-reaction for Pd/PdO:Dx and TiDx targets taken per movable (desorbed) deuteron is found to be 10^{-18}-10^{-16} per 1 D. This figure exceeds the so-called “Jones level” by 5 to 7 orders of magnitude.

The alpha particle emission effect has been observed previously in experiments on D-desorption from the Pd/PdO:Dx [7-9] system and high-current deuterium glow discharge bombardment of the Ti cathode [5]. The origin of energetic alphas still remains puzzling, and further experiments are required in order to shed a light on the mechanism of high energy alpha emission in deuterated solids. In this work we do not consider the alpha emission mechanism. Instead, we are going to discuss possible factors of the DD-reaction enhancement, providing a measurable 3 MeV proton yield.

In this connection, below we show that extrapolation of both DD-reaction cross section and the enhancement factor to very low deuteron energy (E_d ~ 3.0 eV) with a reasonable screening potential U_e = 750 eV, allowed to describe satisfactorily the detected DD-reaction yield in Pd/PdO:Dx target under e-beam excitation. This result strongly supports the theoretical prediction [1,2] with regards to electron excitation of hydrogen subsystem in Pd deuteride.

In order to estimate the DD-reaction rate in the Pd/PdO:Dx target under electron bombardment we use a simple model of the process, taking into account that D-deosrption stimulated by e-beam results in deuterium flux moving toward the Pd/PdO:Dx surface. Thus the moving deuteron flux can be considered a low energy projectile or “deuteron beam,” while the deuterated surface of the Pd/PdO sample we consider a deuterated “target.” The deuteron (D^+) current, estimated via D-desorption rate (see Experimental part) would be of J_d = 0.5 mA/cm^2, while the mean concentration of deuteron at the surface is corresponded to mean D/Pd ratio during e-beam bombardment (<x> ~ 0.15 or $N_d = 1.1 \times 10^{22}$ cm^{-3}).

In order to estimate DD-reaction rate we use a so-called thick target yield expression, normally employed in accelerator physics [3-5], recently developed and modified for lower energy applications [10]:

$$Y_{DD} = J_d N_{eff}(T) \times \int_0^{E_d} f(E)\sigma_{DD}(E)(dx/dE)dE \qquad (1),$$

where J_d – is the deuteron current on target, i.e. in our case, the desorbed deuteron flux from the surface of the Pd/PdO:$D_{<x>}$; $N_{eff}(T) = N_0 \exp(-\varepsilon_d \Delta T / k_B T T_0)$ is the effective deuteron concentration in the target (here N_0 – is the bound deuteron concentration in the target, i.e. at

the Pd/PdO:Dx surface, corresponding to the <x> = D/Pd ~ 0.15±0.05 at T_0 = 290 K, T – is the real target temperature, $\Delta T=T- T_0$, ε_d - is the activation energy of deuteron escape from the target, here ε_d = 0.2 eV= the activation energy of D-diffusion in Pd); $\sigma_{DD}(E)$ – is the "bare" cross-section of DD-reaction (e.g. without any enhancement) and dE/dx – is the deuteron stopping power in the target (here in the Pd); the f(E) - is the enhancement factor, derived from the following equation:

$$f(E) = Y_{exp}(E)/Y_b(E) = \exp[\pi\eta(E)U_e/E] \quad (2),$$

where $Y_{exp}(E)$ – is the total experimental DD-reaction yield at deuteron energy E, taken in the center-of-mass system, $Y_b(E)$ – is the yield deduced with the standard cross-section approximation of Bosch and Halle [11] or bare yield (without taking into account the electron screening in the target); $2\pi\eta(E) = 31.29\ Z^2(\mu/E)^{1/2}$ – is the Sommerfeld parameter (Z – is the charge of the particle, μ- is the reduced mass) and U_e – is the electron screening potential of deuterons in the target. Based on analysis of screening potentials for 60 elements of periodic table [8], it was shown that U_e depends on diffusivity of deuterons in the target and could be determined by semi-empirical formula [10]:

$$U_e = (T/T_0)^{-1/2}[a \ln(y) + b] \quad (3),$$

where a = 145.3 and b=71.2 – are the numerical constants and $y = k \times y_0(J_d/J_0)$, (here $k = \exp(-\varepsilon_d\Delta T/k_B T T_0)$ y_0 = Pd/D at T_0 = 290 K and J_0 = 0.03 mA/cm^2). Substitution of J_d = 0.5 mA/cm^2, T=290 K and <Pd/D> = 6.7 in eq. (3) is resulting in U_e = 750±50 eV. Notice that this screening value falls roughly into the interval limited by Kasagi's (600 eV) [3,4] and Raiola's (800 eV) [12-14] estimates of U_e deduced from the 2.5-10 keV deuteron bombardment results of the Pd/PdO and the Pd targets, respectively.

In order to estimate the DD-reaction yield in the Pd/PDO:DX under e-bombardment, we extrapolate directly to lower energies both the integral $I(E) = \int_0^{E_d} \sigma_{DD}(E)(dx/dE)dE$, (containing linear combination of the bare cross section and stopping power), and the enhancement factor, determined by eq (2) with the U_e ~ 750 eV (Fig. 20).

These extrapolations, as well as substituting of the deuteron flux and effective D-concentration values in eq. (1), allow us to conclude that the DD-reaction rate of ~ 0.01 p/s-cm^2 in 4π steradian could be reached in Pd/PdO:Dx target (with the U_e ~ 750 eV) only in case if the mean kinetic energy of the desorbing deuterons would be of the order of E_d ~ 3-4 eV (i.e. two orders of magnitude above the kT).

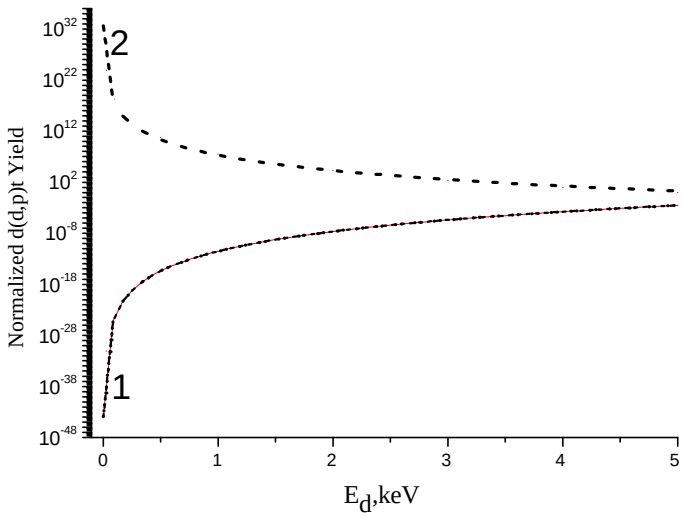

Figure 20. Extrapolation of the bare DD-reaction yield (assuming no enhancement) in Pd/PdO target normalized to that at E_d = 10 keV – (curve 1); and of the enhancement factor (see eq. (2) at screening potential value U_e = 750 eV) - (curve 2), respectively, to very low deuteron energy E_d = 1.0 eV.

Thus, a straight extrapolation of the DD-cross-section and enhancement factor to very low deuteron energy indicate a necessity of the eV range ("hot") deuteron flux desorbed from the Pd/PdODx target in order to provide experimentally measured DD-yield in vacuum under electron beam irradiation. This result strongly supports the theoretical prediction [1,2] with regards to electron excitation of hydrogen subsystem in Pd deuteride. Indeed, the deduced from d(d,p)t reaction rate 3-4 eV deuteron flux serve as a proof of the strong electric field (F ~ 10^8 V/cm) generation within a distance comparable with the lattice parameter (a_0 = 0.39 nm) caused by plasmon formation at the Pd/PdO:Dx surface during e-beam interaction with the D-subsytem of the deuteride.

In contrast to Pd/PdODx data, the results obtained for TiDx target under similar electron irradiation cannot be easy explained by eV deuteron kinetic energies, taking into account only the low energy extrapolation of the linear combination of the DD-reaction cross section and the enhancement factor. The problem is that due to very low D- diffusivity in Ti, the screening potential at the surface of TiDx would be also quite low. Indeed, using eq.(3) with J_d = 0.015 mA/cm^2 and y_0 ~ 2.0 (assuming that at the surface D-concentration is x = D/Ti ~ 0.5 during e-bombardment) one can obtain U_e ~ 70 eV (close to Kasagi's value [4]). At this small screening potential, in order to produce DD-reaction rate of the order of ~ 0.01 p/s-cm^2 , the kinetic energy of deuteron flux (in laboratory system) has to be rather higher, exceeding the value E_d = 1 keV.

The situation could be improved, assuming that main fraction of desorbed deuterium in TiD_x under e-beam irradiation would escape directly from the surface layer (of 1-2 lattice parameter thick), but not from the total 2-4 μm thick area of D-localization. (This, actually, means that the energy transferred by electron beam would be effectively redistributed to the deuterons located

over the top of the TiDx target - sort of inverse population). If, in this case, at the same D-flux $J_d = 0.015$ mA/cm$_2$ the mean residual deuterium concentration at the surface would be x = D/Ti < 0.1 then at $E_d \sim 5$-10 eV and the screening potential $U_e \geq 600$ the deuteron yield, according to eq. (1), become similar to that in Pd/PdO:Dx derived above. It is also possible to speculate that thin TiO_2 strong dielectric layer (in contrast to semi-metallic PdO) always existing on top of the TiDx target can be negatively charged under the electron bombardment. This macroscopic electric field would accelerate D+ ions passing through the surface, thus increasing their kinetic energy from several to hundreds eV. Such a process could certainly increase the yield of DD-reaction in TiDx target. In order to make clear mechanism of high DD-reaction yield in the TiDx target under electron bombardment, further experimental and theoretical studies are required.

5. Conclusions

- Taking into consideration total obtained experimental data, including vacuum experiments with and without e-beam irradiation, we come to the conclusion that electron beam (J ~ 100-300 nA, E = 30 keV) stimulation of the Pd and Ti based deuteride targets (cathodes) surface really can nhance the intensity of the emissions of nuclear charged particles.
- Both the products of DD-reaction (3 MeV protons) and high energy alphas (11-20 MeV) are clear distinguished in e-beam stimulation experiment with the Pd/PdO:D_x and TiD_x targets.
- An important point is that signatures of 3 MeV and energetic alphas are appeared simultaneously at the surface of all (two or three) independent detectors used in the same experiment and covered by metallic foil filters with different stopping ranges/powers. To increase accuracy of measurements the rear detector side background results have been subtracted from the Foreground data obtained at the CR-39 side facing the sample's surface.
- Sequential etching of the detectors 1 and 2 during 7, 14, 21 and 28 hr show an appropriate track diameter shift (an increase), in accordance with the calibration curves obtained by CR-39 proton and alpha accelerator bombardment. This powerful technique allows us to identify unambiguously the emission of 3 MeV protons from DD-reaction as well as indicate a presence of energetic alpha particles with energies in the range 11-20 MeV.
- Total statistics obtained in experiments with the Pd/PdO:Dx heterostructure under e-beam irradiation show 3MeV/DD proton emission intensity in 4 π ster.: $N_p = (1.39 \pm 0.18) \times 10^{-2}$ p/s-cm^2 of the Pd/PdO:Dx sample, with the significance level above the background L = 7.7 σ. The intensity of energetic alphas is found to be: $N_\alpha = (0.71 \pm 0.12) \times 10^{-2}$ α/s-cm^2 of Pd/PdO:Dx sample (the significance level is L = 6.0 σ). The yield of DD-reaction in the Pd/PdO:Dx target under e-beam bombardment, taken only for movable deuterons (the desorbed flux $J_d = 3 \times 10^{15}$ D/s-cm^2) is found to be $\lambda_{DD} \sim 3.3 \times 10^{-18}$ p/D.
- Total statistics obtained in experiments with the TiD_x foils under e-beam irradiation show 3MeV/DD proton emission intensity in 4 π ster.: $N_p = (1.10 \pm 0.23) \times 10^{-2}$ p/s-cm^2 of the TiDx sample. (the significance level above the background is L = 4.74 σ) and alpha intensity $N_\alpha = (0.61 \pm 0.15) \times 10^{-2}$ α/s-cm^2 of the TiD_x sample (the significance level is L = 4.3 σ).

- The yield of DD-reaction in the TiDx target under e-beam bombardment, taken only for movable deuterons (the desorbed flux $J_d = 10^{14}$ D/s-cm^2) is found to be $\lambda_{DD} \sim 1.1x10^{-16}$ p/D.
- No signatures of nuclear emissions have been found in case of Pd/PdO:D_x and TiD_x samples exposed in vacuum at T=290K in absence of e-beam stimulation.
- The rear side of the Pd/PdO:Dx sample (opposite to e-beam irradiated side) show $N_p = (1.68 \pm 0{,}37) \times 10^{-3}$ p/s-cm^2 of the Pd/PdO:Dx sample. (significance L = 4.5 σ) and $N_\alpha = (1.46 \pm 0.27) \times 10^{-3}$ α/s-cm^2 of the Pd/PdO:Dx sample. (significance L = 5.5 σ). These values are 5-8 times less than charged particle emissions intensities from the e-beam bombarded side.
- The results presented here could be even more statistically significant; however, the batch of CR-39 track detectors used in this study has been irradiated by weak fast neutron flux on the route to Moscow from USA, most probably in an airport security facility. As a result the background level in the track diameter range of interest (4-8 μm) was found to be 4-5 times above the usual 4-8 μm track diameter background, which normally shows N < 10 track/cm^2. This important feature further convinces us that the CR-39 batches should be transported personally on board aircraft and cannot be placed in a baggage facility.
- Data analysis has been performed for Pd/PdO:Dx target. Extrapolation of both DD-reaction cross section and the enhancement factor to very low deuteron energy ($E_d \sim 3.0$ eV) with a reasonable screening potential $U_e = 750$ eV, allowed to describe satisfactorily the detected DD-reaction yield in Pd/PdO:Dx target under e-beam excitation. This result strongly supports the theoretical prediction [1,2] with regard to electron excitation of hydrogen subsystem in the Pd deuteride.

References

1. Yu. Tyurin and I. Chernov, Int. J. Hydrogen Energy **27**, 829 (2002).
2. V. Silikin, I.Chernov et al, Phys.Rev.B, **76**, 245105 (2007).
3. H. Yuki, J. Kasagi , A. G. Lipson et al, JETP Lett, **68**(11) , 785, (1998).
4. J. Kasagi, H.Yuki, T. Baba, et al, J. Phys. Soc. Jpn., v. **71**(12), 2881 (2002).
5. A.G. Lipson, A.S. Roussetski, A.B. Karabut and G.H. Miley., JETP, **100**, 1175 (2005).
6. A.G. Lipson, A.S. Roussetski and E.I. Saunin, “Analysis of #2 W. Williams’s detector after SPAWAR/Galileo type electrolysis experiment”, Proc. of 8-th Int. Workshop on Anomalies in Hydrogen/Deuterium Loaded Metals, 13-18 Oct., 2007, Catania, Italy.
7. A.G. Lipson, A.S. Roussetski et al., “Observation of long-range alpha-particles during deuterium/hydrogen desorption from Au/Pd/PdO:D(H) heterostructure”, Bulletin of the Lebedev Physical Institute (Russian Academy of Sciences)] **#10**, pp. 22-29 (2001).
8. A.G. Lipson, G.H. Miley, A.S. Roussetski, Trans. Amer. Nuclear. Soc.. **88**, 638 (2003).
9. A.G. Lipson et al, ICCF-12 proc., Yokohama, Japan (2005).
10. A.G. Lipson et al, High Energy Chemistry, **42**(4), 361 (2008).
11. H.S. Bosch and G.M. Halle, Nuclear. Fusion **32**, 611, (1992).
12. F. Raiola, P. Migliardi, L. Gang, et al. Phys. Lett B **547**, 193 (2002).
13. F. Raiola, L. Gang, C. Bonomo et al, Europhys. J.A**19**, 283 (2004).
14. F. Raiola, B. Burchard, Z. Fulop et al, J. Phys. G: Nucl. Part. Phys., **31**, 1141 (2005).